Journal of the Korean Ceramic Society (2020) 57:206–212
https://doi.org/10.1007/s43207-020-00019-y

ORIGINAL ARTICLE

Crack-free TiO_2 films prepared by adjusting processing parameters via liquid phase deposition technique

Jie Li[1] · Hai-Yan Xu[1,2] · Ai-Guo Wang[1] · Feng-Jun Zhang[1,2] · Dao-Sheng Sun[1] · Won-Chun Oh[3]

Received: 30 October 2019 / Revised: 25 November 2019 / Accepted: 9 December 2019 / Published online: 3 February 2020

Abstract
TiO_2 thin films with controllable morphology and grain size were prepared via a liquid phase deposition (LPD) technique. The effects of the processing parameters including the $(NH_4)_2TiF_6$ concentration, solution pH, and $(NH_4)_2TiF_6$:H_3BO_3 molar ratio on the grain size and morphology of the films were investigated. The prepared samples were characterized by X-ray diffraction, scanning electron microscopy, and ultraviolet–visible spectroscopy. The results showed that the deposition parameters significantly affected the growth and nucleation velocities of the crystalline grains, which resulted in the formation of TiO_2 films with different morphologies and grain sizes. The capillary stress among the grains of the film, which resulted in the cracking of the film, depended on the size of the grains. Thus, the cracking of the LPD-derived TiO_2 films could be mitigated by adjusting the deposition parameters.

Keywords TiO_2 thin film · Morphology control · Size control · Crack-free

1 Introduction

As one of the most promising semiconductors, titanium dioxide (TiO_2) has been extensively utilized in organic pollutant degradation [1, 2], solar energy conversion [3–7], and photoelectrochemical water splitting [8–11]. Although TiO_2 shows good stability, non-toxicity, low cost, and high photocatalytic activity, its wide bandgap (3.2 eV for anatase) limits its applications in visible light [12, 13]. Owing to their recycling ability, TiO_2 thin films deposited on various substrates have gained immense attention over the past 2 decades [14, 15].

Liquid phase deposition (LPD) is a novel soft wet chemical technique for preparing various metal oxide films. Unlike other film-preparation techniques, LPD does not require vacuum, high temperature, expensive equipment, and special substrates [16, 17]. However, TiO_2 thin films prepared by the LPD method are highly susceptible to cracking [18]. TiO_2 thin films undergo cracking during drying because of the presence of capillary stress.

Gong et al. [19] reported that the cracking of TiO_2 films can be mitigated by doping them with tungsten. At the tungsten content of 5% (at. %) the cracking of the film could be eliminated completely. Zhang et al. [20] reported that the deposition of WO_3 on TiO_2 films result in the formation of flower-like WO_3 crystals, and the cracks in LPD TiO_2 films can be completely eliminated by coating the surface of TiO_2 with WO_3. The morphology of TiO_2 films can be tailored by adjusting the experimental conditions. Cheng et al. [21] reported that the substrate type affects the structural properties of TiO_2 thin films. The surfaces of TiO_2 films deposited on Si substrates are rougher than those of the films deposited on glass. Lei et al. [22] reported that TiO_2 monolayer films show an acicular rod-like surface morphology, whereas SnO_2−TiO_2 bilayer composite films exhibit a network-like surface morphology with aggregated tiny SnO_2 nanosheets. Huang et al. [23] reported that the deposition rate and surface roughness of TiO_2 films can be controlled by adjusting

✉ Hai-Yan Xu
xuhaiyan@ahjzu.edu.cn

✉ Won-Chun Oh
wc_oh@hanseo.ac.kr

[1] Anhui Key Laboratory of Advanced Building Materials, Anhui Jianzhu University, Hefei, Anhui 230022, People's Republic of China

[2] Key Laboratory of Functional Molecule Design and Interface Process, Anhui Jianzhu University, Hefei, Anhui 230601, People's Republic of China

[3] Department of Advanced Materials Science and Engineering, Hanseo University, Seosan 31962, Korea

the H_3BO_3 concentration. The results showed that high boric acid concentrations neutralized HF in the reactive solution, thereby generating films with high surface roughness and large particle sizes.

In this study, we investigated the relationship between the deposition processing parameters (precursor concentration, solution pH, and precursor molar ratio) and the microstructure of TiO_2 films prepared by LPD. The cracking of the films could be mitigated by controlling their morphology by varying the deposition conditions.

2 Materials and experiment

2.1 Chemicals

All the chemicals used in this study including ammonium fluorotitanate (95% purity), boric acid (99.8% purity), hydrofluoric acid, hydrochloric acid, acetone, and absolute ethanol were purchased from Sinopharm Chemical Reagent Co., Ltd (China) with analytical grade and were used without any further purification. Deionized (DI) water was used to prepare the reaction solution.

2.2 Preparation of TiO_2 thin films

The LPD method was used for preparing the thin films. Prior to the preparation of the TiO_2 thin films, the glass substrates (2 cm × 2 cm) were washed sequentially with acetone, absolute ethanol, and DI water for 10 min. Dilute HF (1:4 in volume) was used to etch the glass substrates for 1–3 min. The substrates were then rinsed with DI water and dried in air. The pH of the mixture of $(NH_4)_2TiF_6$ and H_3BO_3 was adjusted by adding diluted HCl. The pre-treated substrates were then horizontally immersed (with the surface upside down) in the prepared solution in a beaker. The beaker was then heated at 80 °C for 3 h. The substrates were then taken out, rinsed with DI water, and dried in air at 60 °C.

2.3 Characterization

The phase compositions of the products were analyzed by X-ray diffraction (XRD, Germany Bruker Science, Co. Ltd Bruker D8 ADVANCE) with monochromatized Cu–K radiation (λ = 0.1541874 nm). The morphologies of the products were examined using scanning electron microscopy [SEM, JEOL JSM-7500F (Japan)] at an acceleration voltage of 10 kV. The transmittance of the products was measured using ultraviolet–visible spectroscopy (UV–Vis, UV-8000S Yuanxi Instrument Co. Ltd, China).

3 Results and discussion

3.1 Phase structure analysis of the TiO_2 films

The XRD patterns of the samples with different raw material molar ratios are shown in Fig. 1. All the samples showed three sharp diffraction peaks corresponding to the (101), (004) and (200) [24] planes of anatase TiO_2 (JCPDS No. 21-1272). This indicates that the prepared samples were anatase titanium dioxide and showed good crystallinity. The samples showed no impurity peaks. No significant difference was observed in the shapes of patterns (a), (b), and (c) and their peak positions. This indicates that the $(NH_4)_2TiF_6$: H_3BO_3 molar ratio did not affect the crystallinity of the obtained films.

3.2 Effect of the precursor concentration on the TiO_2 films

The morphologies of the TiO_2 thin films obtained using 0.2 and 0.1 M $(NH_4)_2TiF_6$ at pH = 2.0 and $(NH_4)_2TiF_6$:H_3BO_3 = 1:1.5 are shown in Fig. 2a and b, respectively. The surfaces of both the films showed a large number of cracks. These cracks resulted in the warping and peeling off of the films from the substrate (Fig. 2a2), which severely limited the practical applications of the films. Anatase TiO_2 films prepared by LPD generally show cracks [25, 26]. The optical microscopy observations revealed that the films showed cracking only after complete drying and not after cooling and washing with DI water. This indicates that the films cracked because of

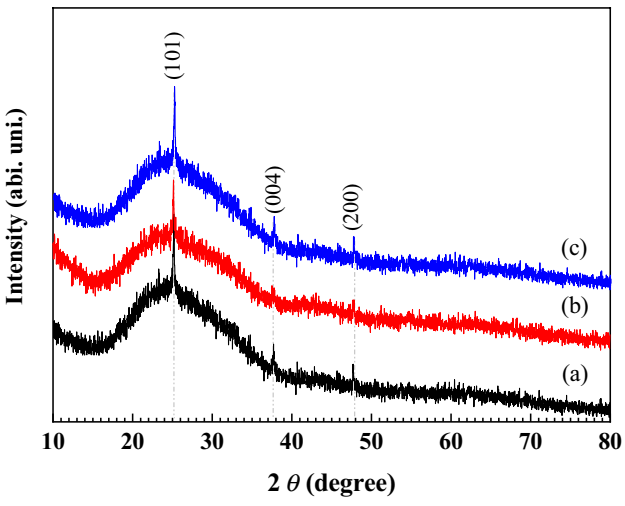

Fig. 1 XRD patterns of the thin films with different $(NH_4)_2TiF_6$: H_3BO_3 molar ratios. **a** 1:1.5; **b** 1:2, and **c** 1:3

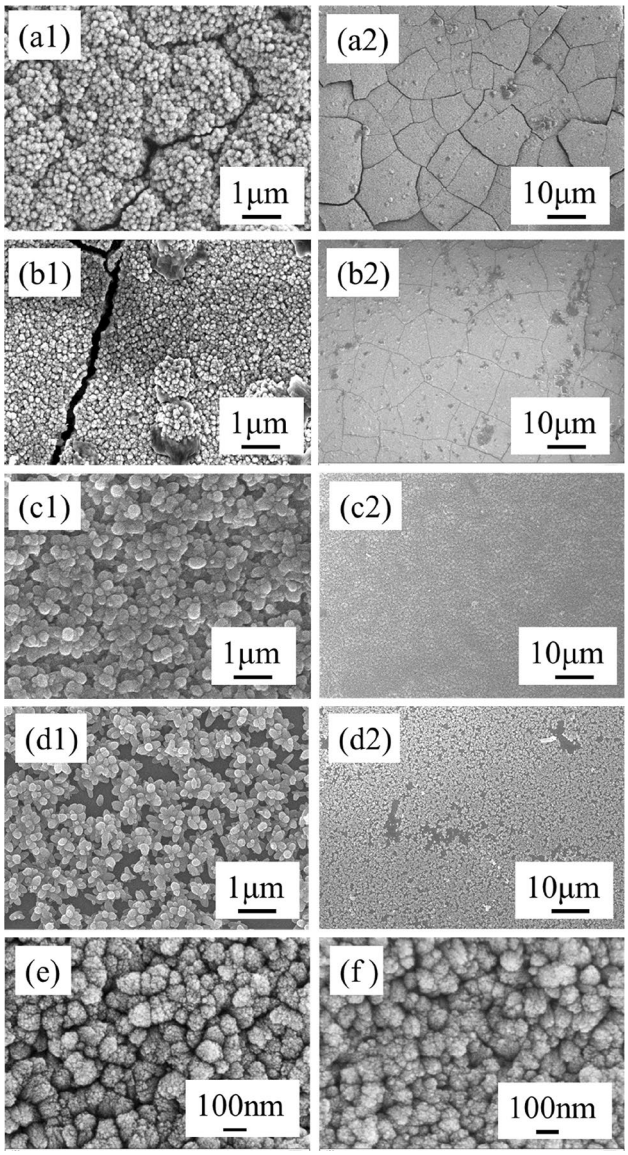

Fig. 2 Surface morphologies of TiO_2 thin films prepared using different $(NH_4)_2TiF_6$ concentrations: **a** 0.20 M; **b** 0.10 M; **c** 0.05 M; **d** 0.03 M and the 100,000 × magnification micrographs of the TiO_2 thin films with the $(NH_4)_2TiF_6$ concentrations of **e** 0.20 M, **f** 0.10 M

the mismatch in their coefficients of thermal expansion with that of the substrate [18]. According to the Laplace equation [27],

$$\Delta P = -2\gamma \cos\theta / r, \tag{1}$$

where γ is the surface tension and r is the pore radius. When the pore size was less than 10 nm, the capillary stress, which caused the shrinkage of the films was significant. The grain size of films prepared from liquid solutions can be controlled by varying their growth and nucleation velocities. These velocities can be controlled by adjusting the ion concentration of the solution. The ion concentration can be simply adjusted by varying the concentration of the deposited solution. Therefore, crack-free TiO_2 films are obtained at low solution concentrations.

Figure 2c shows the SEM image of the film prepared using 0.05 M $(NH_4)_2TiF_6$. The surface of the film was dense and uniform. The film was composed of sub-micron-sized spherical clusters along with nano-sized grains (~ 80 nm). Figure 2d shows the SEM image of the film prepared using 0.03 M $(NH_4)_2TiF_6$. The film showed flower-like morphology. There were some blanks among these flowers, and the surface density was low. The grains were elongated, but the size did not increase. This phenomenon occurred as follows [28]:

$$\left[TiF_6\right]^{2-} + nH_2O \leftrightarrow \left[TiF_{6-n}(OH)_n\right]^{2-} + nH^+ + nF^-, \tag{2}$$

$$\left[TiF_{6-n}(OH)_n\right]^{2-} + (6-n)H_2O \leftrightarrow \left[Ti(OH)_6\right]^{2-} + (6-n)HF, \tag{3}$$

$$H_3BO_3 + 4HF \leftrightarrow BF_4^- + H_3O^+ + 2H_2O, \tag{4}$$

$$\left[Ti(OH)_6\right]^{2-} + 2H^+ \leftrightarrow TiO_2 + 4H_2O. \tag{5}$$

These reactions proceeded smoothly towards the right when the concentration of $[TiF_6]^{2-}$ was high (0.1 M and 0.2 M). During the nucleation process, large quantities of raw materials were supplied and the solutions reacted quickly because of their high ionic concentrations. In this case, the nucleation velocity was much higher than the growth velocity, therefore, a large amount of TiO_2 grains were accumulated. However, the size of the grains did not increase, and the pore size remained small. The ΔP value increased according to Eq. (1), resulting in the generation of cracks. The thin film prepared using 0.2 M $(NH_4)_2TiF_6$ showed severe cracking as compared to the one prepared using 0.1 M $(NH_4)_2TiF_6$. This is because the higher $(NH_4)_2TiF_6$ concentration resulted in smaller grains and pores. Fine clusters with the sizes of about 60–80 nm composed of a large number of fine grains with the sizes of less than 10 nm were observed (Fig. 2e, f). On the contrary, in the case of the low ion concentration (0.03 M), the nucleation velocity was low and the difference between the growth velocities of different crystal planes increased because of the lack of growth units. Therefore, single grains grew into short rods with the size of ~ 100 nm. These short rods shared one end and aggregated to form flower-like particles because of the lack of nucleation sites.

The thin films prepared with different ion concentrations showed significantly different optical transmittance owing to their different microstructures. The films prepared using the high concentration solutions (0.10 and 0.20 M) were

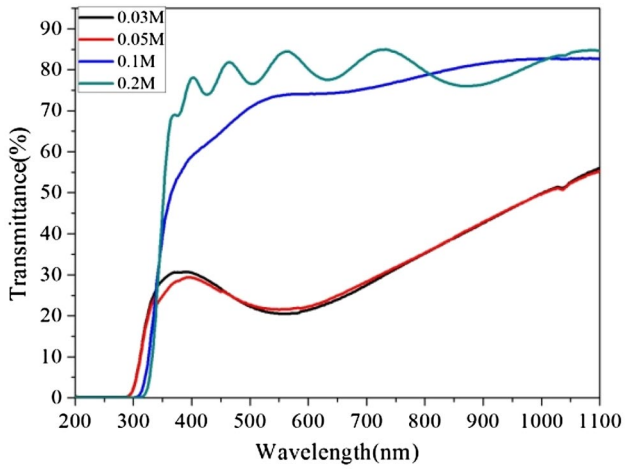

Fig. 3 UV–Vis transmittance spectra of the films with different $(NH_4)_2TiF_6$ concentrations

transparent to visible light. However, the films prepared using the low concentration solutions (0.03 and 0.05 M) were white and opaque to visible light. Figure 3 shows the transmittance of the films prepared at different ionic concentrations. The transmittances of the films (in the visible light range of the spectrum) with the solution concentrations of 0.03 and 0.05 M were less than 30% (Fig. 3c, d), while those of the films with the solution concentrations of 0.10 and 0.20 M were higher than 70% (Fig. 3a, b). It can be observed that the cracks on the 0.10 and 0.20 M films showed no significant effect on their transmittance (> 70%). The low transmittance of the 0.03 and 0.05 M films can be attributed to light scattering. This is consistent with the microstructure observations of the films (Fig. 2). The grain size of the 0.10 and 0.20 M films was less than 10 nm, which is much smaller than the visible light wavelength. Therefore, these films were transparent to visible light. However, the grain size of the 0.03 and 0.05 M films was ~ 100 nm, which is of the same order of magnitude as the wavelength of visible light. The films acted as inhomogeneous media for visible light. When photons hit the sub-micrometer TiO_2 grains, serious scattering occurred, which resulted in a low transmittance. Moreover, it can be observed that there were interference fringes on the 0.20 M film. This indicates that the thickness and optical constants of this film remained constant. When the film was irradiated with photons, light interfered on the surface and interference fringes were generated.

The 0.1 and 0.2 M TiO_2 thin films showed absorption edges at ~ 306 and ~ 310 nm. On the other hand, the 0.03 and 0.05 M films showed absorption edges at ~ 300 nm. The absorption edge of the films prepared at high concentrations showed a red shift. This can be explained by the surface effect of nano-materials. The high-concentration films showed crystalline grains with sizes less than 10 nm. The high surface energy induced lattice distortions in the films, which caused variations in the bond length of the films.

3.3 Effect of solution pH on the TiO_2 films

The reaction ion concentration of the deposition solution was affected not only by the concentration of the raw materials, but also by the pH of the solution and the molar ratio of the raw materials. Therefore, the effect of the solution pH on the size and morphology of the TiO_2 films was investigated. Figure 4 shows the SEM images of the samples prepared with 0.03 M $(NH_4)_2TiF_6$ and 0.045 M H_3BO_3 at different pH values. A flower-like TiO_2 thin film was obtained at the solution pH of 1.5 (Fig. 4a). The grain size of this film was about 200 nm. The grains accumulated at particular sites and formed flower-like clusters. Furthermore, the flower-like clusters grew sparsely on the surface of the substrate and a discontinuous film was observed. At the solution pH of 2.0, the grain size of the obtained film decreased to about 100 nm, and the micromorphology of the film transformed to sphere-like clusters composed of ~ 100-nm grains. With a

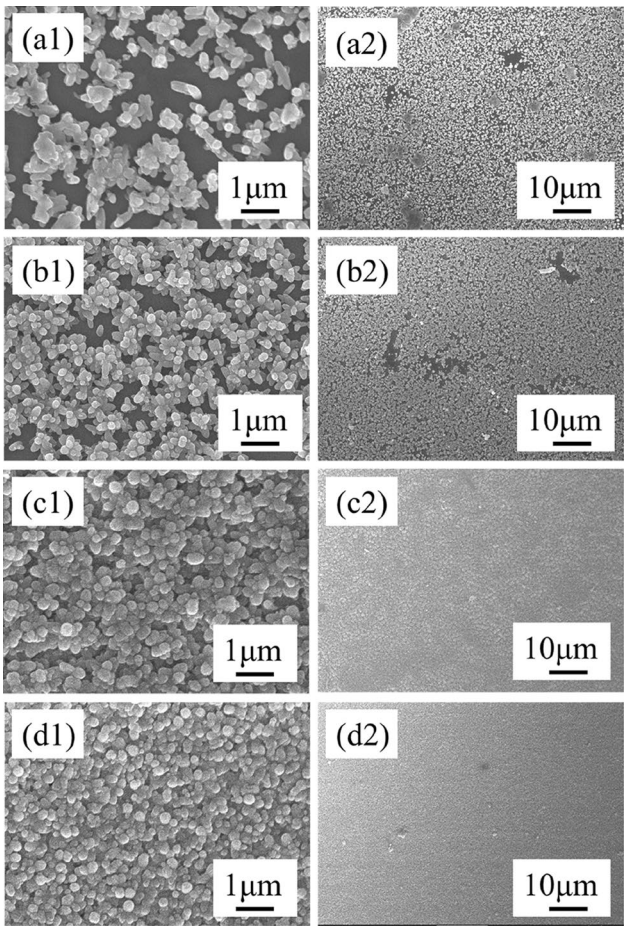

Fig. 4 Surface morphologies of the TiO_2 thin films prepared at different pH values. **a** 1.5; **b** 2.0; **c** 2.3; **d** 2.5

further increase in the solution pH, the grain size of the films decreased further and the density of the films increased. As can be observed from Fig. 4c the film prepared with the solution pH of 2.3 was uniform and dense and the grain size was only about 80 nm. The morphology of the film with the solution pH of 2.5 is shown in Fig. 4d. No significant difference was observed in the morphologies of films shown in Fig. 4d and c. The grains agglomerated into spheres with a size of ~ 150 nm and the film was dense and compact. The grain size was less than 80 nm. The density of the TiO_2 film on the surface of the substrate increased with an increase in the pH from 2 to 2.3. The morphology of the film changed gradually from sparse flower-like to dense and compact clusters with an increase in the solution pH.

This phenomenon can also be explained by reactions (2), (3), (4), and (5). According to reaction (2), when pH value was low (1.5 and 2), there were less OH^- ions in the solution but more H^+ ions. As a result, the process of TiO_2 formation was disadvantageous. When the pH value was relatively high (2.3 and 2.5), there were a large number of OH^- ions in the solution and reaction (2) was more likely to proceed to the right. Therefore, the film was continuous and consisted of a large amount of TiO_2. Moreover, during the growth of the thin film, the amount of OH^- increased and the grains tended to nucleate. The film was very compact and continuous (Fig. 4c, d).

The UV–Vis transmittance spectra of the samples are shown in Fig. 5. The absorption edges of all the as-prepared TiO_2 thin films appeared at ~ 300 nm. The effect of the solution pH on the transmittance of the films was not significant (Fig. 5). However, the transmittance of the film with the lowest pH (1.5) was the highest. This can be attributed to the very low TiO_2 content and the discontinuous growth of this film. This film also showed the leakage of light during the testing process. In some areas, photons irradiated the glass substrate. At the same time, the transmittance of the glass substrate (not the TiO_2 thin film) was investigated. Hence, its transmittance was relatively high.

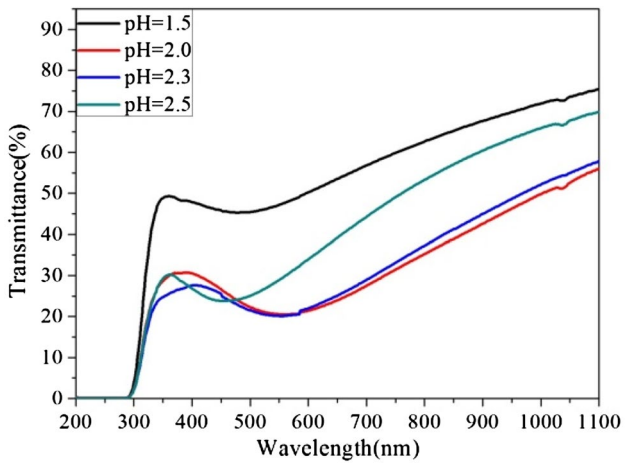

Fig. 5 UV–Vis transmittance spectra of the films with different pH values

3.4 Effect of the raw material molar ratio on the TiO_2 films

The grain size and morphology of TiO_2 films can be tailored by controlling the raw material molar ratio. Figure 6 shows the morphologies of the films prepared with different $(NH_4)_2TiF_6$:H_3BO_3 ratios (1:1.5, 1:2, and 1:3). The 1:1.5 film (Fig. 6a) was composed of micro clusters of ~ 100-nm gains. The substrate was not completely covered with the clusters. In other words, this film was not fully dense (Fig. 6a). The grain size of the 1:2 thin film (~ 80 nm) was smaller than that of 1:1.5 film (Fig. 6b). The fine grains grew and agglomerated into microspheres. However, the compactness of the obtained film did not improve. The 1:3 film was dense and homogeneous (Fig. 6c). The film was compact and consisted of fine grains. Therefore, the grain size of the films decreased with an increase in the amount of H_3BO_3. The morphology of the films changed from micro-sized flowers to spheres and then to compact nano-sized grains with an increase in the ratio of H_3BO_3.

According to reactions (2), (3), (4), and (5), H_3BO_3 acted as a F^- scavenger [28]. As can be observed from Fig. 6, the films became denser and more uniform with an increase in

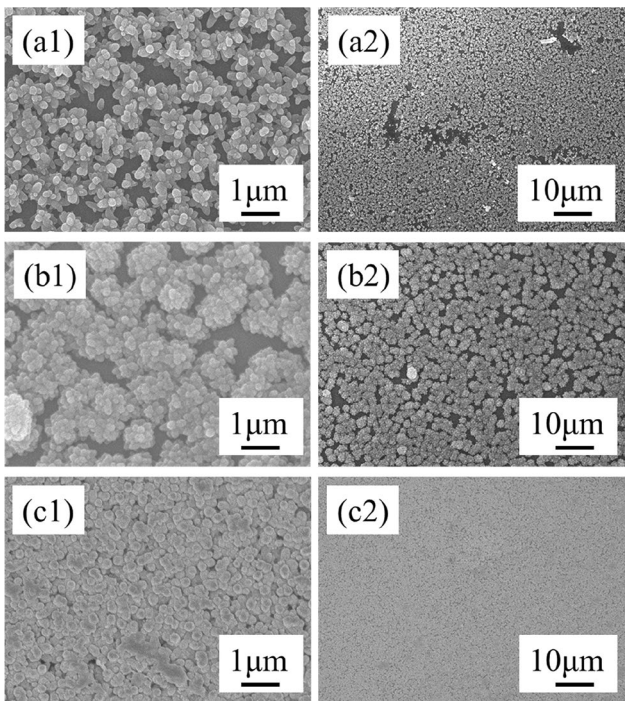

Fig. 6 Surface morphologies of the as-prepared TiO_2 thin films with different $(NH_4)_2TiF_6$:H_3BO_3 molar ratios. **a** 1:1.5; **b** 1:2; **c** 1:3

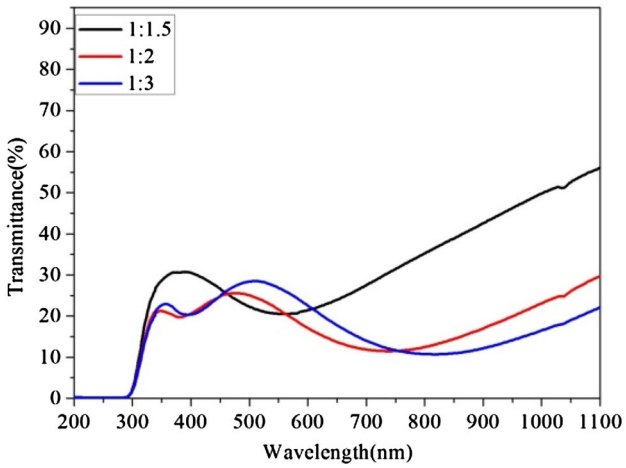

Fig. 7 UV–Vis transmittance spectra of the films with different $(NH_4)_2TiF_6$:H_3BO_3 molar ratios

the H_3BO_3 concentration. This is because at high H_3BO_3 concentrations, the solution consisted of a few F^- ions. As a result, reaction (4) proceeded towards the right. Reactions (2), (3), and (5) proceeded towards the right when the F^- content was low. A large number of crystal nuclei were formed rapidly on the substrate at high H_3BO_3 concentrations. The process of nucleus formation consumed most of the $[Ti(OH)_6]^{2-}$ ions, which caused the reaction to quickly reach the equilibrium state before the growth of the nuclei. As a result, the obtained film was uniform and compact.

Figure 7 shows the transmittance spectra of the thin films. All the samples showed adsorption edges at 300 nm. No significant difference was observed between the curve shapes and transmittances of the samples. As can be observed from Fig. 6, the scattering phenomenon was caused by the submicron cluster of nanograins. The size of the clusters exactly matched with the wavelength detected. Therefore, the transmittances of thin films were relatively low. All the three curves showed slight interference fringes, indicating the uniformity of the thin films.

4 Conclusion

In summary, TiO_2 films with controllable grain size and morphology were prepared using the LPD technique. The grain size and morphology of the TiO_2 films were controlled by adjusting the deposition parameters including the raw material concentration, solution pH, and raw material molar ratio. Here, the ion concentration, which was controlled by varying the deposition parameters, affected the nucleation and growth velocities of the TiO_2 films, which in turn affected the grain size of the films. The capillary stress among the grains was controlled accordingly. Therefore, crack-free LPD-derived TiO_2 films were obtained by simply adjusting the deposition parameters. At very low nucleation velocities (lower concentration, 0.03 M; or lower pH, 2.0; or higher ratio, 1:1), the grains tended to grow and the morphology of the film transformed to flower-like. At very high nucleation velocities (higher concentration, 0.1 M and 0.2 M), the grain size decreased and the film became dense. However, numerous micro-scale cracks were observed on the film because of its large capillary stress.

Acknowledgements This work was financially supported by Outstanding Young Talents Support Program in Colleges and Universities (gxyqZD2016150), National Natural Science Foundation of China (51778003 and 51578004), and Major Projects of Natural Science Research in Anhui Colleges and Universities (KJ2018ZD050).

References

1. X.D. Yang, Y.Q. Wang, Z.S. Wang, X.Z. Lv, H.X. Jia, J.H. Kong, M.H. Yu, Preparation of CdS/TiO_2 nanotube arrays and the enhanced photocatalytic property. Ceram. Int. **42**, 7192–7202 (2016)
2. W. Liang, J. Li, Y. Jin, Photo-catalytic degradation of gaseous formaldehyde by TiO_2/UV, Ag/TiO_2/UV and Ce/TiO_2/UV. Build. Environ. **51**, 345–350 (2012)
3. A.M. Bakhshayesh, M.R. Mohammadi, D.J. Fray, Controlling electron transport rate and recombination process of TiO_2 dye-sensitized solar cells by design of double-layer films with different arrangement modes. Electrochim. Acta **78**, 384–391 (2012)
4. J. Wan, Y. Lei, Y. Zhang, Y. Leng, J. Liu, Study on TiO_2 photoelectrode to improve the overall performance of dye-sensitized solar cells. Electrochim. Acta **59**, 75–80 (2012)
5. A.S. Shikoh, Z. Ahmad, F. Touati, R.A. Shakoor, S.A. Al-Muhtaseb, Optimization of ITO glass/TiO_2 based DSSC photoanodes through electrophoretic deposition and sintering techniques. Ceram. Int. **43**, 10540–10545 (2017)
6. C. Xu, Y.J. Zhong, Y.N. Zheng, W.Y. Huang, C. Jin, B.B. Xu, R.Q. Yao, Z.D. Feng, Micromixing-assisted preparation of TiO_2 films from ammonium hexafluorotitanate and urea by liquid phase deposition based on simulation of mixing process in T-shaped micromixer. Ceram. Int. **45**, 11325–11334 (2019)
7. G.Y. Roh, H.S. Sung, Y.C. Lee, S.E. Lee, Study on optical characteristics of nano hollow silica with TiO_2 shell formation. J. Korean Ceram. Soc. **56**, 98–103 (2019)
8. H. Wu, Z. Zhang, Photoelectrochemical water splitting and simultaneous photoelectrocatalytic degradation of organic pollutant on highly smooth and ordered TiO_2 nanotube arrays. J. Solid State Chem. **184**, 3202–3207 (2011)
9. Z. Zhang, M.F. Hossain, T. Takahashi, Photoelectrochemical water splitting on highly smooth and ordered TiO_2 nanotube arrays for hydrogen generation. Int. J. Hydrogen. Energ. **35**, 8528–8535 (2010)
10. M. Frites, S.U.M. Khan, Visible light active hydrogen modified (HM)-*n*-TiO_2 thin films for photoelectrochemical splitting of water. Electrochem. Commun. **11**, 2257–2260 (2009)
11. A. Boonserm, C. Kruehong, V. Seithtanabutara, A. Artnaseaw, P. Kwakhong, Photoelectrochemical response and corrosion behavior of CdS/TiO_2 nanocomposite films in an aerated 0.5 M NaCl solution. Appl. Surf. Sci. **419**, 933–941 (2017)

12. D. Wu, M. Long, Realizing visible-light-induced self-cleaning property of cotton through coating N-TiO_2 film and loading AgI particles. ACS. Appl. Mater. Inter. **3**, 4770–4774 (2011)
13. C.X. Lei, Z.D. Feng, H. Zhou, Visible-light-driven photogenerated cathodic protection of stainless steel by liquid-phase-deposited TiO_2 films. Electrochim. Acta **68**, 134–140 (2012)
14. B. Dudem, L.K. Bharat, J.W. Leem, D.H. Kim, J.S. Yu, Hierarchical Ag/TiO_2/Si forest-like nano/micro-architectures as antireflective, plasmonic photocatalytic, and self-cleaning coatings. ACS. Sustain. Chem. Eng. **6**, 1580–1591 (2017)
15. Y. Yu, J. Wang, J.F. Parr, Preparation and Properties of TiO_2/fumed silica composite photocatalytic materials. Procedia. Eng. **27**, 448–456 (2012)
16. Y. Ding, C. Yang, L. Zhu, J. Zhang, Photoelectrochemical activity of liquid phase deposited TiO_2 film for degradation of benzotriazole. J. Hazard. Mater. **175**, 96–103 (2010)
17. M. Mallak, M. Bockmeyer, P. Löbmann, Liquid phase deposition of TiO_2 on glass: systematic comparison to films prepared by sol–gel processing. Thin Solid Films **515**, 8072–8077 (2007)
18. B. Ma, G.K. Goh, J. Ma, T.J. White, Growth kinetics and cracking of liquid-phase-deposited anatase films. J. Electrochem. Soc. **154**, D557–D561 (2007)
19. J. Gong, C. Yang, W. Pu, J. Zhang, Liquid phase deposition of tungsten doped TiO_2 films for visible light photoelectrocatalytic degradation of dodecyl-benzenesulfonate. Chem. Eng. J. **167**, 190–197 (2011)
20. M. Zhang, C.Z. Yang, W.H. Pu, Y.B. Tan, K. Yang, J.D. Zhang, Liquid phase deposition of WO_3/TiO_2 heterojunction films with high photoelectrocatalytic activity under visible light irradiation. Electrochim. Acta. **148**, 180–186 (2014)
21. X. Cheng, K. Gotoh, Y. Nakagawa, N. Usami, Effect of substrate type on the electrical and structural properties of TiO_2 thin films deposited by reactive DC sputtering. J. Crys. Growth. **491**, 120–125 (2018)
22. C.X. Lei, X. Huang, X. Liu, A.S. Wang, G.S. Zhang, D.L. Peng, Photoelectrochemical performances of the SnO_2−TiO_2 bilayer composite films prepared by a facile liquid phase deposition method. J. Alloy. Compd. **692**, 227–235 (2017)
23. J.J. Huang, S.L. Ou, C.F. Hsu, X.Q. Shen, The effect of boric acid concentration on the TiO_2 compact layer by liquid phase deposition for dye-sensitized solar cell. Appl. Surf. Sci. **477**, 7–14 (2019)
24. M.C. Marchi, S.A. Bilmes, C.T.M. Ribeiro, E.A. Ochoa, M. Kleinke, F. Alvarez, A comprehensive study of the influence of the stoichiometry on the physical properties of TiOx films prepared by ion beam deposition. J. Appl. Phys. **108**, 064912 (2010)
25. M. Mahé, J.M. Heintz, J. Rödel, P. Reynders, Cracking of titania nanocrystalline coatings. J. Eur. Ceram. Soc. **28**, 2003–2010 (2008)
26. H. Pizem, C.N. Sukenik, U. Sampathkumaran, A.K. McIlwain, M.R. De Guire, Effects of substrate surface functionality on solution-deposited titania films. Chem. Mater. **14**, 2476–2485 (2002)
27. F. Fresno, R. Portela, S. Suárez, J.M. Coronado, Photocatalytic materials: recent achievements and near future trends. J. Mater. Chem. A. **2**, 2863–2884 (2014)
28. Y. Gao, Y. Masuda, K. Koumoto, Microstructure-controlled deposition of $SrTiO_3$ thin film on self-assembled monolayers in an aqueous solution of $(NH_4)_2TiF_6 - Sr(NO_3)_2 - H_3BO_3$. Chem. Mater. **15**, 2399–2410 (2003)